Metal-Free cAMP-Dependent Protein Kinase Can Catalyze Phosphoryl Transfer

Oksana Gerlits,[†] Amit Das,[†] Malik M. Keshwani,[‡] Susan Taylor,[‡] Mary Jo Waltman,[§] Paul Langan,[†] William T. Heller,[†] and Andrey Kovalevsky*,[†]

[†]Biology and Soft Matter Division, Oak Ridge National Laboratory, Oak Ridge, Tennessee 37831, United States
[‡]Departments of Chemistry/Biochemistry & Pharmacology, University of California San Diego, La Jolla, California 92093, United States
[§]Bioscience Division, Los Alamos National Laboratory, Los Alamos, New Mexico 87545, United States

Ⓢ *Supporting Information*

ABSTRACT: X-ray structures of several ternary product complexes of the catalytic subunit of cAMP-dependent protein kinase (PKAc) have been determined with no bound metal ions and with Na^+ or K^+ coordinated at two metal-binding sites. The metal-free PKAc and the enzyme with alkali metals were able to facilitate the phosphoryl transfer reaction. In all studied complexes, the ATP and the substrate peptide (SP20) were modified into the products ADP and the phosphorylated peptide. The products of the phosphotransfer reaction were also found when ATP-γS, a nonhydrolyzable ATP analogue, reacted with SP20 in the PKAc active site containing no metals. Single turnover enzyme kinetics measurements utilizing ^{32}P-labeled ATP confirmed the phosphotransferase activity of the enzyme in the absence of metal ions and in the presence of alkali metals. In addition, the structure of the *apo*-PKAc binary complex with SP20 suggests that the sequence of binding events may become ordered in a metal-free environment, with SP20 binding first to prime the enzyme for subsequent ATP binding. Comparison of these structures reveals conformational and hydrogen bonding changes that might be important for the mechanism of catalysis.
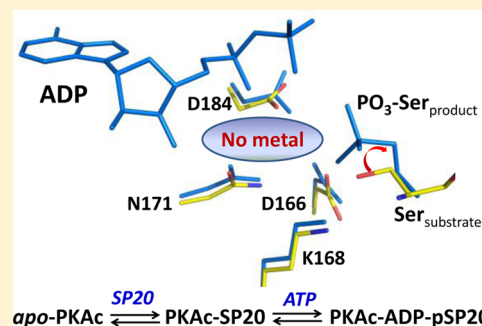
Signaling through the phosphorylation of proteins by protein kinase enzymes plays an important role in the regulation of a variety of physiological responses. ATP-dependent protein kinases are phosphotransferases that deliver the γ-phosphoryl group from the nucleotide to the hydroxyl of a serine, threonine, or tyrosine of a substrate protein to produce the phosphomonoester and ADP products. Among the diverse serine/threonine protein kinase family, cAMP-dependent protein kinase A (PKA) has served as an extensively studied model for investigations of the mechanism of all kinases.[1−3] *In vivo*, the inactive PKA holoenzyme consists of two catalytic (C) and two regulatory (R) subunits. An increase in cAMP concentration, due to β-adrenergic stimulation of cells, activates PKA by providing four cAMP molecules that bind to the R subunits, which in turn dissociate from the C subunits (referred to here as PKAc) that had been bound in an inactive holoenzyme state.[4]

Experiment and theory have demonstrated that the catalytic cycle of PKAc involves several structural and dynamic steps. *apo*-PKAc is in a dynamically uncommitted open conformation, showing very little conformational exchange on the microsecond to millisecond time scale.[5−7] Catalysis initiates when MgATP binds to produce the binary PKAc−MgATP complex, which causes PKAc to transition to an intermediate conformation that itself is partially rate-limiting at physiological $Mg^{2+}$ concentrations (∼0.5 mM).[6−10] Substrate binding to PKAc−MgATP produces the ternary complex in which PKAc adopts the closed conformation necessary for chemical catalysis,[11] although the ternary Michaelis complex may cycle between the closed and intermediate conformations multiple times before phosphorylation actually take place.[7] Following the dissociation of the phosphorylated product from the active site, MgADP is released, which is concurrent with the enzyme's return to the open conformation and is the second potentially rate-limiting step.[5,12]

Divalent metal cations are thought to play important roles throughout the catalytic cycle. Early studies pointed to a fundamental role for divalent metal cations in PKAc activity.[13,14] The PKAc active site possesses two metal-binding sites (M1 and M2; Figure 1). The occupancy of one site is sufficient for activity, whereas occupancy of the second site improves the affinity to both ATP and ADP. Indeed, in the absence of divalent cations in solution, no nucleotide binding or phopshotransferase activity has been detected.[15] Early reports suggested that at low physiological concentrations Mg^{2+} binds first to the M1 site, coordinated by β- and γ-phosphates of ATP.[16−18] The M2 site, coordinated by α- and γ-phosphates of
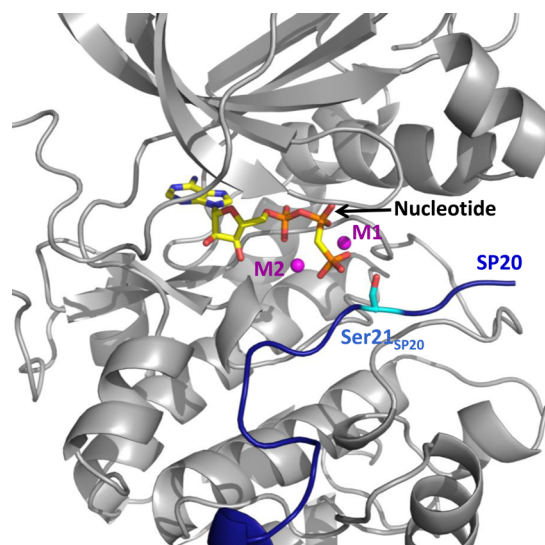
Figure 1. A close-up view of the PKAc structure in cartoon representation (PDB ID 4IAC, Gerlits et al.[25]). The two Mg^{2+} cations at sites M1 and M2 are represented by magenta spheres, while a nucleotide is shown in stick representation colored by atom type. SP20 peptide is colored blue, and the substrate's Ser21 is shown in stick representation colored by atom type.

ATP, becomes occupied at higher metal concentrations.[10,17,19] When both sites are occupied at high metal concentrations, ADP release becomes the rate-limiting process.[9]

Our understanding of the role of metal in the catalytic cycle has been challenged recently by X-ray crystallography studies that revealed that M2 rather than M1 is occupied at low Mg^{2+} concentrations.[20] Computational studies also supported greater involvement of M2 in chemical catalysis than M1.[21−23] Further, although Mg^{2+} is considered to be the physiologically relevant metal based on its relatively high concentration in cells,[15,24] it has been demonstrated that all other divalent alkaline earth metals (Ca^{2+}, Sr^{2+}, and Ba^{2+}) support the phosphoryl transfer in complexes with the 20-residue substrate analogue peptide SP20.[25] This unexpected result contradicted early kinetic measurements showing no PKAc activity in the presence of Ca^{2+} or Sr^{2+} using the Kemptide (LRRASLG) peptide substrate and no nucleotide binding when Ba^{2+} was present.[15]

The fact that ATP binding to PKAc is undetectable in the absence of divalent metals[15] leads us to propose that high substrate binding affinity can produce PKAc activity in a metal-free environment. SP20 has nanomolar binding affinity to PKAc.[26,27] Here, X-ray crystallography and single turnover enzyme activity measurements with [γ-^{32}P]ATP were used to determine whether PKAc can bind ATP and transfer the γ-phosphoryl group to Ser21 of SP20 in the absence of free divalent metal ions. The results show that a stable PKAc−SP20 binary complex forms that can coordinate ATP to form the catalytically active ternary complex. The results reinforce the conclusions of several computational studies[21−23] that suggest that the primary role of the metal ions is to lower the transition state energy through electrostatic effects, rather than bond making or breaking during the chemical reaction. Importantly, the current study provides a major revision to our understanding of the role of the different components involved in the catalytic cycle of PKAc.

MATERIALS AND METHODS

General Information. Pseudosubstrate peptide SP20 (TTYADFIASGRTGRRASIHD; residues 5−24 of the heat-stable PKAc inhibitor PKI, where positions 20 and 21 have been mutated to alanine and serine) was custom-synthesized by and purchased from Biomatik (Wilmington, Delaware, USA). ATP, as the disodium salt, and ATP-γS (in which sulfur replaces one of the terminal oxygen atoms), as a tetralithium salt, were purchased from Sigma-Aldrich (St. Louis, Missouri, USA). Protein purification supplies were purchased from GE Healthcare (Piscataway, New Jersey, USA). Crystallization reagents were purchased from Hampton Research (Aliso Viejo, California, USA).

Protein Expression and Purification. His$_6$-tagged recombinant mouse PKAc was expressed in *Escherichia coli* using Luria-Bertani (LB) media at 16−24 °C for 16−20 h. The recombinant enzyme was purified by affinity chromatography using HisTrap fast-flow chromatography columns supplied by GE Healthcare. The enzyme was then buffer-exchanged with 50 mM 2-(N-morpholino)ethanesulfonic acid (MES)−NH_4OH, 250 mM NH_4Cl, 2 mM dithiothreitol (DTT) at pH 6.5 on a desalting column. For PKAc−Na_2ADP−pSP20, the enzyme was buffer-exchanged with 50 mM MES−NaOH, 250 mM NaCl, 2 mM DTT, pH 6.5. Isoforms of PKAc, which differ by the number and positions of autophosphorylated residues, were not separated, without any obvious effect on crystallization of the ternary complexes.

Enzyme Activity Measurements. The activity of PKAc in the presence and absence of monovalent and divalent metals was measured in the single turnover regime utilizing ^{32}P-labeled ATP (ATP*) and SP20 as substrates. The kinetics measurements were carried out in the presence of 40 μM ethylenediaminetetraacetic acid (EDTA) at 25 °C. The common reaction mix contained 50 mM 3-(N-morpholino)-propanesulfonic acid (MOPS), pH 7.4, 10 μM SP20, 2 μM enzyme, 1 mM ATP, and ATP radiolabeled with ^{32}P in the γ-position (ATP*, specific activity 500−1500 cpm/pmol) in a final volume of 20 μL. The various metal ions used were Mg^{2+}, Ca^{2+}, K^+, and Na^+ at final concentrations of 1 mM. The reaction was carried out as a time course experiment with 0, 60, and 300 min.

The reaction was initiated by adding 10 μL of the mix containing ATP, ATP*, and PKAc to 10 μL of the solution with metal (or no metal) and SP20. The γ-phosphoryl group of ATP* containing the radioactive marker was transferred to Ser21 of SP20 during the measurements. After each time-point, the reaction was quenched with 90 μL of 30% acetic acid. A 50 μL portion of the quenched reaction was then spotted on p81 phosphocellulose paper, washed 3 times for 5 min each with 5% phosphoric acid and once with acetone, air-dried, and counted on a liquid scintillation counter. The background counts were subtracted from the measured values. The difference in counts (total counts minus background counts) was divided by the activity of ^{32}P ATP (cpm/pmol) to get the concentration of the phosphorylated pSP20 product.

Crystallization and Data Collection. For crystallization trials, PKAc was concentrated to 8−12 mg/mL. The ternary and binary complexes with no metals, Na^+ or K^+, ATP (or ATP-γS), and SP20 were made before crystallization trials were set up. For the metal-free binary PKAc−SP20 complex, the enzyme solution was mixed with the peptide substrate, and $(NH_4)_2$EDTA was added to reach a final concentration of 20

mM. For the metal-free ternary complexes, the enzyme solution was combined with a premade solution of Na$_2$ATP in 50 mM MES−NH$_4$OH, 250 mM NH$_4$Cl, 1 M (NH$_4$)$_2$EDTA, and 2 mM DTT at pH 6.5, and then peptide substrate was added. The molar ratio of PKAc/ATP(or ATP-γS)/SP20 was kept at 1:5:5. The final concentration of EDTA in the ternary complex solutions was 50 mM, and that of ATP was 5 mM. EDTA has about 10^5 higher affinity than ATP for Mg^{2+} and other divalent and trivalent metal ions, so it should chelate any trace amounts of metal present. For PKAc−Na$_2$ADP−pSP20 and PKAc−K$_2$ADP−pSP20, the enzyme solutions were mixed with Na$_2$ATP and SP20. Crystals were grown in sitting drop microbridges or in 9-well glass plates using well solutions consisting of 100 mM MES−NH$_4$OH, pH 6.5, 5 mM DTT, 15−20% PEG 4000, and 150 mM NaCl for PKAc−Na$_2$ADP−pSP20 or 50 mM KCl for PKAc−K$_2$ADP−pSP20 at 4−14 °C. PKAc−SP20 crystallized in 15−20% PEG3350.

Structure Determination and Refinement. X-ray crystallographic data were collected from frozen crystals at 100 K for all complexes. The data sets were collected on a Rigaku HomeFlux system, equipped with a MicroMax-007 HF generator and Osmic VariMax optics. The diffraction images were obtained using an RAXIS-IV++ image-plate detector. For the binary PKAc−SP20 complex, a 1.7 Å resolution diffraction data set was collected at the Advanced Photon Source on the beamline 19-ID. Diffraction data were collected, integrated, and scaled using HKL3000 software suite.[28] The structures were refined using SHELX-97[29] for PKAc−ADP−pSP20, PKAc−Na$_2$ADP−pSP20, and PKAc−K$_2$ADP−pSP20, and PHENIX[30] for PKAc−SP20, PKAc−ADP−psSP20. A summary of the crystallographic data and refinement is given in Supporting Table 1, Supporting Information. Similar to our previous observations,[20,25] all of the structures were of isoform 2 and contained three post-translationally phosphorylated residues, Ser139, Thr197, and Ser338.

The structure of the ternary complex of PKAc with 2Mg^{2+}, ADP, and phosphorylated peptide pSP20 (PDB ID 4IAD)[25] was used as a starting model for structure determination. Structures were built and manipulated with program *Coot*,[31] whereas the figures were generated using the *PyMol* molecular graphics software (v.1.5.0.3; Schrödinger LLC). The absence of metal ions was confirmed by the lack of electron density at the M1 and M2 sites in the $F_O − F_C$ difference electron density maps. The presence of metal ions (Na$^+$ and K$^+$) was established by ensuring that the strongest peaks in $F_O − F_C$ maps with metals omitted and $2F_O − F_C$ maps with metals present corresponded to positions M1 and M2 and by checking that the coordination spheres of seven ligands were present around the metal ions. Differences in coordination geometries were also used to distinguish between metal ions. As an example, in the case of PKAc−Na$_2$ADP−pSP20, we determined that the metal was sodium because the coordination around the metal ions differed from that found in our previously published product complex with magnesium, and because no magnesium was used during the sample preparation. Potassium has almost twice the number of electrons as sodium or magnesium; therefore, K$^+$ was identified by a much larger electron density peak than that for the smaller sodium metal. The representative electron densities in the active sites of PKAc−ADP−psSP20, PKAc−Na$_2$ADP−pSP20, and PKAc−K$_2$ADP−pSP20 complexes are shown in Supporting Figures 1 and 2, Supporting Information, while coordination of metals in Na$^+$ and K$^+$ complexes are given

in Supporting Table 2 and Supporting Figure 3, Supporting Information.

The structures have been deposited to the Protein Data Bank and were assigned the following PDB codes: 4IB3 for PKAc−ADP−pSP20 (ternary complex of PKAc with products ADP and phosphorylated SP20); 4O21 for PKAc−ADP−psSP20 (ternary complex of PKAc with products ADP and thiophosphorylated SP20); 4IB0 for PKAc−Na$_2$ADP−pSP20 (ternary complex of PKAc with two sodium cations and products ADP and phosphorylated SP20); 4IB1 for PKAc−K$_2$ADP−pSP20 (ternary complex of PKAc with two potassium cations and products ADP and phosphorylated SP20); and 4O22 for PKAc−SP20.

■ RESULTS

Enzyme Activity. In the presence of Mg^{2+} and Ca^{2+}, the phosphotransfer reaction was already at equilibrium after 60 min, and the amount of the product remained unchanged after 300 min (Figure 2). The PKAc activity was significantly lower
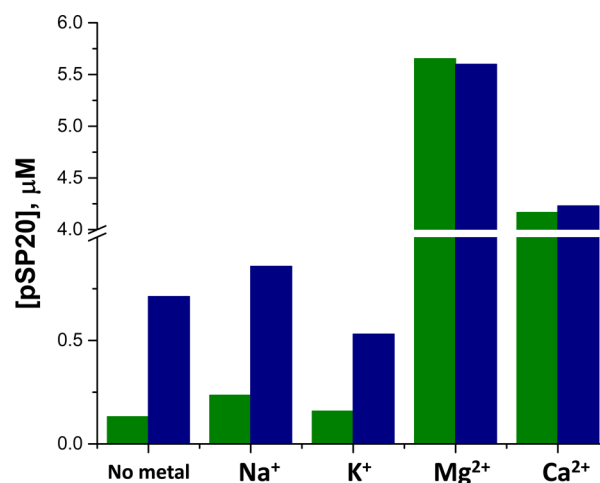

Figure 2. Amounts of pSP20 synthesized by PKAc at two time points of 60 (green bars) and 300 min (blue bars) in the presence of no metal, Na$^+$, K$^+$, Mg^{2+}, and Ca^{2+}.

when no metal or monovalent metals were present in the reaction mixture, producing ∼2% and 5−10% of the phosphorylated product after 60 and 300 min, respectively. The enzyme's activity is substantially impaired, but not abolished, without divalent metal ions relative to its performance with Mg^{2+} and Ca^{2+}. Interestingly, metal-free PKAc was as active as that with Na$^+$ or K$^+$, indicating that the alkali metal ions do not play a role in the phosphoryl transfer.

Ternary Complexes with ADP, pSP20, and No Metal. The active site of PKAc−ADP−pSP20 is shown in Figure 3a and is free of bound metal. Contrary to previous studies, the phosphotransfer reaction has occurred, and the products, ADP and pSP20, are trapped (Figure 3b). The positions of the products are stabilized by a network of potential hydrogen bonds and water-mediated interactions. The PKAc−ADP−psSP20 structure is very similar to PKAc−ADP−pSP20, with the only structural difference confined to the glycine-loop region (Supporting Figure 4, Supporting Information). This flap-like hairpin structure spans residues 49−57, contains three glycine residues, and acts as a lid for the catalytic site cavity. The flap is slightly more compact in PKAc−ADP−psSP20 due to a 1.5 Å shift of residues 52−54 away from the alternate
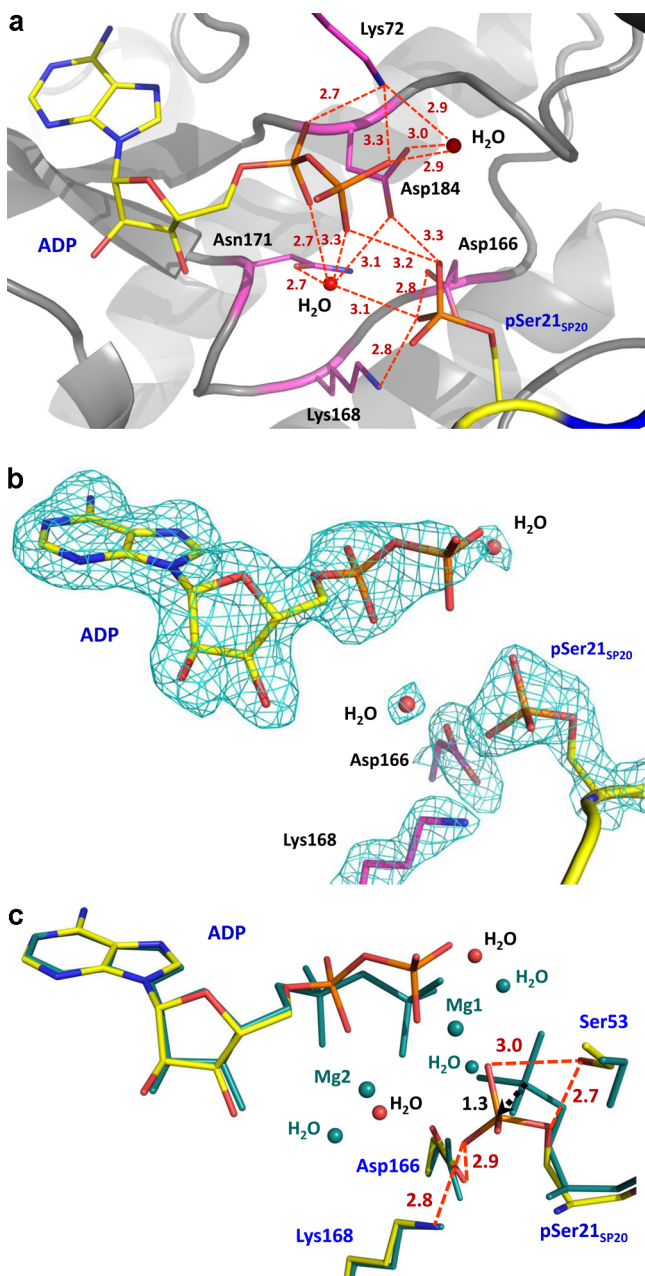
Figure 3. (a) A close-up view of the enzyme active site in PKAc–ADP–pSP20 product complex showing ADP, phosphorylated pSer21$_{SP20}$, and the enzyme's residues important for catalysis. Possible hydrogen bonds are represented as red dashed lines. (b) Electron density for the active site components ADP, Asp166, Lys168, and pSer21$_{SP20}$ contoured at the 1.5σ level (the contour level is 1.0σ for ADP to show the phosphates). (c) Superposition of the active sites from PKAc–ADP–pSP20 and PKAc–Mg$_2$ADP–pSP20. The distance between the phosphorus atoms in pSer21$_{SP20}$ residues is shown as black dashed arrow, indicating that the product phosphate moved over 1 Å in the metal-free structure toward Asp166 and Lys168 relative to its position in the magnesium structure. Distances are in Å.

conformation of thiophosphate side chain of psSer21$_{SP20}$. As a consequence, a hydrogen bond does not form between the thiophosphate of psSer21$_{SP20}$ and the side chain OH of Ser53 in the glycine-rich loop in PKAc–ADP–psSP20, unlike in PKAc–ADP–pSP20 and the divalent metal-bound ternary product complexes reported previously.[25] Instead, a new hydrogen bond forms between the amide of Gly52 and the carbonyl of Gly55
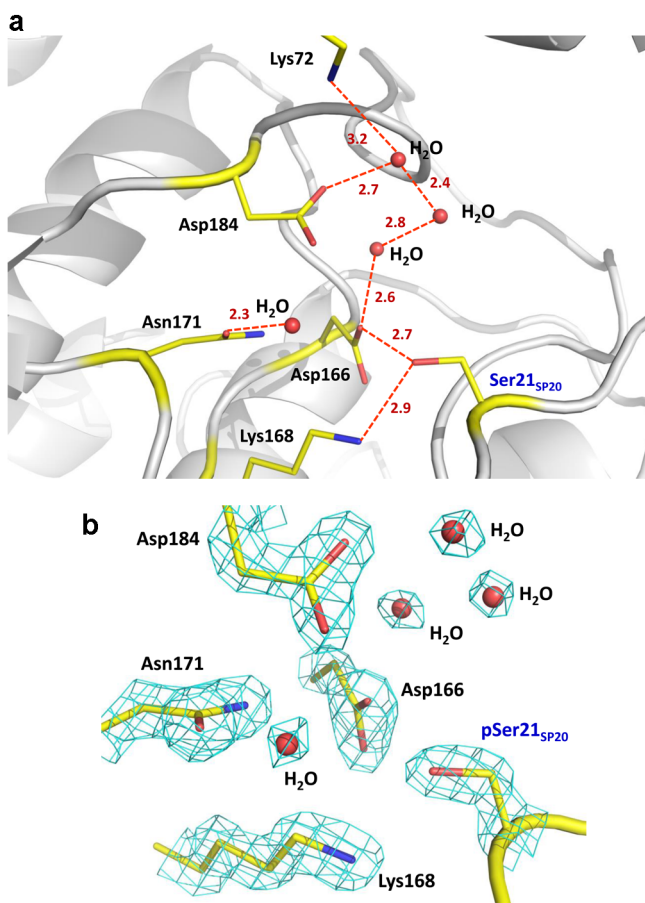
of PKAc–ADP–psSP20. This 2.8–3.2 Å long hydrogen bond is found in all product complexes containing divalent metals, indicating that, in addition to being flexible as a whole, the flap is also internally flexible.

The β-phosphate of ADP is quite mobile in both metal-free ternary complexes, having B factors of the order of 70–100 Å^2, whereas the pSer21$_{SP20}$ phosphate and psSer21$_{SP20}$ thiophosphate groups are less mobile, having the B factors of the order of 40–50 Å^2. The pSer21$_{SP20}$'s phosphate group is drawn 1.3 Å closer to the active site residues relative to its position in PKAc–Mg$_2$ADP–pSP20,[25] possibly due to the lack of metal ions. This shift is accomplished without a rotation around the Oγ–Cβ bond of the phosphorylated serine (Figure 3c). The pSer21$_{SP20}$ side chain position creates hydrogen bonds with Asp166 and Lys168 in the metal-free PKAc–ADP–pSP20 structure that are absent from the metal–product complexes. Similar hydrogen bonds form with the sulfur atom of psSer21$_{SP20}$ in one of the alternate conformations.

Ternary Complexes with ADP, pSP20, and Excess Na$^+$ and K$^+$. Metal was observed in both the M1 and M2 sites of the PKAc–Na$_2$ADP–pSP20 and PKAc–K$_2$ADP–pSP20 structures with the phosphotransfer products despite the fact that ionic radii of Na$^+$ (1.0 Å) and K$^+$ (1.38 Å) are significantly larger than that of Mg^{2+} (0.7 Å). The active sites of the Na$^+$ and K$^+$ structures are very similar to PKAc–Mg$_2$ADP–pSP20, including the position and orientation of the ADP and pSer21$_{SP20}$ phosphate groups.[25] Further, the pSer21$_{SP20}$ phosphoryl groups are both oriented away from Asp166 and Lys168, which maintains a 2.5–2.6 Å long hydrogen bond to the OH of Ser53 in the glycine-rich loop (Supporting Figure 5, Supporting Information), which compares well with the 2.8 Å distance in PKAc–Mg$_2$ADP–pSP20. Ser53's side chain (Cβ–Oγ bond) is rotated by almost 180° from its conformation in PKAc–Mg$_2$ADP–pSP20, which allows it to face Phe54 and to make a hydrogen bond with the imidazole of His23$_{SP20}$.

The octahedral geometry around the magnesium ions in PKAc–Mg$_2$ADP–pSP20 does not form in PKAc–Na$_2$ADP–pSP20 or PKAc–K$_2$ADP–pSP20. Na$^+$ and K$^+$ have seven ligands at M1 and M2, consistent with preferences of alkali metals for coordination numbers above six. Here, the seventh ligands are water molecules. The metal ion coordination spheres, metal–ligand distances, and metal hydration in the alkali metal complexes differ from the magnesium product complex (Supporting Table 2 and Supporting Figures 3 and 5, Supporting Information). As was observed in the Ca^{2+}, Sr^{2+}, and Ba^{2+} complexes, the terminal phosphoryl groups on ADP and pSer21$_{SP20}$ are slightly (~0.5 Å) father away from each other compared with their locations in PKAc–Mg$_2$ADP–pSP20. These different active site geometries may be explained by the larger Na$^+$ and K$^+$ ionic radii, as well as the higher coordination numbers.

Binary Complex with SP20 and No Metal. The active site of the PKAc–SP20 complex is shown in Figure 4a. The intact peptide substrate is bound to the enzyme, and the unmodified OH group of Ser21$_{SP20}$ can be seen (Figure 4b). No density that can be attributed to metal ions is present in either the M1 or M2 sites. The side chain of Ser21$_{SP20}$ is rotated toward PKAc, forming hydrogen bonds with Asp166 and Lys168. In contrast, the Cβ–Oγ bond is rotated by ~140° toward the bulk solvent in the metal-free and metal-bound product complexes (Figure 5). The absence of a nucleotide causes PKAc to adopt a conformation that is intermediate between the apo-form open conformation and the closed
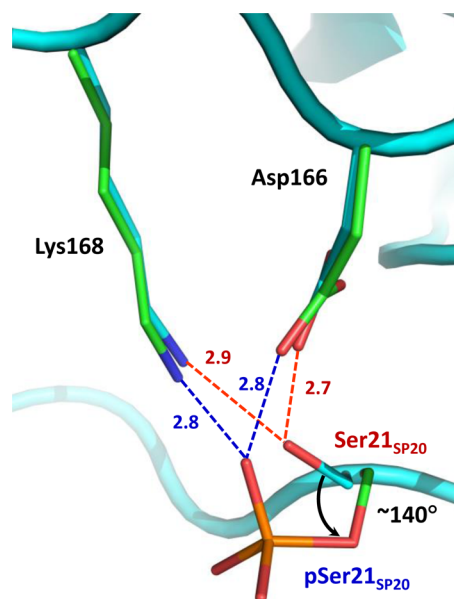
Figure 5. Superposition of PKAc−SP20 and PKAc−ADP−pSP20 showing the conformation of the $C\beta-O\gamma$ bond of the Ser21$_{SP20}$ side chain before and after the phosphotransfer reaction. Hydrogen bonding formed by Ser21$_{SP20}$ and pSer21$_{SP20}$ with active-site residues Asp166 and Lsy168 is shown as dashed lines. Distances are in Å.

Figure 4. (a) A close-up view of the enzyme active site in PKAc−SP20 binary complex showing intact Ser21$_{SP20}$ and the enzyme's residues important for catalysis. Possible hydrogen bonds are represented as red dashed lines. (b) Electron density for the active site residues, Ser21$_{SP20}$, and water molecules contoured at the 2.0σ level (the contour level is 1.5σ for H_2O). Distances are in Å.

conformation of the ternary complexes. There is a significant shift of the glycine-rich loop (4 Å for Ser53) upward toward the α-helix in the small lobe of PKAc, displacing residues 76 through 84 from the positions adopted in PKAc−ADP−pSP20 and PKAc−Mg$_2$ADP−pSP20 (Supporting Figure 5, Supporting Information).

■ DISCUSSION

The phosphotransferase activity of PKAc is highly dependent on divalent metal ions. It has been previously shown that PKAc binds divalent metals weakly in the absence of a nucleotide, with $K_D > 1$ mM.[13] Similarly, PKAc does not bind ATP without divalent metals.[15] For a short peptide substrate Kemptide, which has moderate binding affinity, PKAc shows activity with only a few types of divalent metal ions.[15] In contrast, PKAc is capable of transferring the γ-phosphoryl group from ATP to the SP20 peptide substrate, which binds tightly to PKAc, when any alkaline earth metal is present.[25] Further, the results presented here conclusively demonstrate that phosphotransfer can take place without divalent metals (Figure 2), although the enzyme activity is greatly diminished. Interestingly, alkali metal ions have no effect on the kinase activity with SP20, because the amount of pSP20 was measured to be similar in the reactions with no metal, Na$^+$, and K$^+$, raising the possibility that these cations may not be present when the phosphotransfer takes

place. The only other kinase known to function without divalent metal ions is the pseudokinase CASK, whose activity is actually inhibited by divalent cations in the order of Mg^{2+} > Mn^{2+} > Ca^{2+}.[32] It is important to note that previous studies have investigated removal of key functionalities from the PKAc active site, albeit by mutagenesis, and also failed to completely abolish the enzyme's activity. The single mutation variants Lys72Ala, Lys168Ala, and Asp166Ala showed greatly diminished phosphotransferase activity, being below 1% that of the wild-type protein,[33,34] much like the present results. These three residues form hydrogen bonds with the phosphate groups of ATP and substrate,[16,17,20,24,25] and their primary roles in the reaction are to facilitate the phosphoryl transfer.[1] Substitutions of the other active site residue, Ser53, had no effect on the steady-state phosphorylation of the substrate Kemptide, indicating that it does not participate in the reaction.[35]

In the current study, the single-turnover enzyme activity measurements quantitatively determined the amounts of pSP20 that were phosphorylated by metal-free PKAc, although SP20 phosphorylation was not detected in steady-state kinetics experiments. While the measurements did not provide a reaction rate constant and utilized reaction incubation times much longer than steady-state techniques,[19] the results demonstrate phosphorylation of a substrate in the absence of divalent cations. In contrast, no kinase activity was detected via steady-state kinetics measurements when PKAc was reacted with Kemptide in the metal-free environment or in the presence of Na$^+$ or K$^+$. The ability of PKAc to phosphorylate SP20, but not Kemptide, in metal-free conditions may be related to the extremely high binding affinity (~100 nM) of SP20, whose sequence is based on the heat-stable protein kinase inhibitor (PKI).[26,27] The productive binding of a substrate and MgATP to the *apo*-active site of PKAc has been considered formally random,[19] but almost simultaneous,[7] with the preferred initial binding of MgATP.[36] Based on the present results, we propose that the sequence of binding events

may become ordered in a metal-free environment, with SP20 binding first to prime the enzyme for subsequent ATP binding. The PKAc−SP20 binary complex is stable and has an intermediate, partially closed, conformation (Supporting Figure 6, Supporting Information), suggesting that such a sequence of events is possible. Previously, the X-ray structure of the similar binary complex containing phosphorylated SP20 has been reported.[37] In addition, studies on the pH dependence of the kinetic mechanism demonstrated that pSP20 bound prior to MgADP in the reaction in the direction of MgADP phosphorylation at pH 6.5,[38] which supports our hypothesis. An equimolar mixture of ATP and Mg^{2+} contains predominantly the $MgATP^{2-}$ complex, with low but appreciable amounts of ATP^{4-} and $HATP^{3-}$.[39] $HATP^{3-}$, in which one of the γ-phosphoryl oxygens is protonated, has the ionization constant (pK_a) of 6.5;[40] therefore, it is expected that 50% of ATP will be in the form of $HATP^{3-}$ in the studies reported here. The PKAc active site has a net negative charge, which would repel the bare ATP^{4-} more strongly than it would the singly protonated $HATP^{3-}$. Consequently, it is reasonable to propose that the monoprotonated nucleotide species $HATP^{3-}$ is the reactive molecule that binds to the PKAc−SP20 binary complex to generate a catalytically viable ternary complex that subsequently reacts to produce the product complex PKAc−ADP−pSP20 observed in our crystal structure.

Cook et al.[19] previously showed that KCl increases the K_M of MgATP and the K_i of MgADP at physiological magnesium concentrations, when one Mg^{2+} ion binds to the PKAc active site. The same phenomenon was observed for Na_2SO_4, which eliminates competitive inhibition of PKAc by chloride ions. These observations can be explained by the alkali metal binding to the second metal site at concentrations of ∼100 mM, thereby increasing the counterion charge to 3 and resulting in the diminished affinity of ATP and ADP for the active site. The product structures PKAc−Na_2ADP−pSP20 and PKAc−K_2ADP−pSP20 demonstrate that alkali metals can bind to PKAc even though alkali metals have extremely low ATP-binding constants (∼100 mM).[41] However, the single turnover kinetics data indicate that the rate of SP20 phosphorylation is about the same in the presence of Na^+ or K^+ as it is in the absence of any metals. We propose that Na^+ and K^+ may not come to the PKAc active site bound to ATP but instead diffuse opportunistically into the PKAc−ADP−pSP20 complex after the reaction takes place.

Recent molecular dynamics simulations of the Michaelis complexes reported that the OH group of a substrate peptide's serine adopts a substrate-dependent conformation. In Kemptide, the OH was rotated toward Asp166, whereas in SP20, it is pointed away from Asp166 into the bulk solvent.[42] In PKAc−SP20, the side chain of $Ser21_{SP20}$ is rotated toward Asp166 and Lys168, forming hydrogen bond interactions with the aspartate's carboxylic and the lysine's amino groups. The same "inward" conformation of the hydroxyl was found in earlier PKAc complexes that mimicked the transition state and product structures.[34,43] Intriguingly, in PKAc−ADP−pSP20 and in all product complexes with metals[25] the hydroxyl moiety of pSP20 adopts a different "outward" conformation, being rotated out by ∼140° relative to its position in PKAc−SP20 (Figure 5). Conformational flexibility of the substrate's OH may be an important factor in the mechanism of phosphoryl transfer.

Enzymes are remarkable catalysts that can dramatically lower the energy barrier that a chemical reaction has to overcome in several ways including lowering the reaction entropy by bringing together and correctly positioning reactants (which improves the chance of collision between the reactants relative to solution) and lowering the activation energy of the reaction by distorting reactants and stabilizing the transition state through the creation of a favorable environment.[44,45] Each part of an enzyme, whether it be the catalytic residues, cofactors, or moving ensembles of residues (loops or domains), can be involved, but the reaction pathway is not dramatically altered relative to solution chemistry. In the case of PKAc, computational studies suggest that metals stabilize the phosphotransfer reaction's transition state having the pentacoordinated γ-phosphorus.[21−23,46,47] Our observations of structures of PKAc and its activity when no free metal is present indicate that divalent cations do not constrain the active site geometrically to promote the reaction and are not engaged in the chemical transformation. Instead, they provide a favorable electrostatic environment for the reaction thereby lowering the energy of the transition state.

It follows that the absence of PKAc bound metals dramatically increases the reaction energy barrier for the tightly bound SP20, but the reaction still proceeds because the enzyme promotes a favorable reduction in reaction entropy through the binding of reactants. Baseline catalytic activity has also been reported for other enzymes (which may be reduced by orders of magnitude) in the absence of seemingly critical functionalities. For example, NADH oxidase from *Thermus thermophilus* showed detectable activity, albeit reduced by about 2 orders of magnitude, in the absence of flavin adenine mononucleotide, which is an essential electron acceptor.[48] Similarly, the metalloenzyme cytidine 3′,5′-cyclic monophosphate phosphodiesterase can catalyze the hydrolysis reaction with no divalent metal cofactor present.[49] For these other enzymes, it is likely that a less optimal pathway has been found to facilitate the reaction. However, the results presented here for PKAc suggest that we should not discount the general significance of the simple reduction in reaction entropy provided by enzymes when they bind reactants, that is, the "entropy trap" effect remains an important aspect of enzyme catalysis.

■ CONCLUSIONS

We have provided new evidence that PKAc is active in the presence of other divalent metal cations, rather than just with the previously assumed physiological Mg^{2+} cofactor. This raises the important possibility that Ca^{2+} may also be a physiological cofactor. Further, we have demonstrated that PKAc is active in the absence of metals, which is only the second example of such a kinase. This result has profound implications for our understanding of the role that metals play in PKAc catalysis, expanding on our previous work showing activity in the presence of all alkali earth metals.[25] Excitingly, the metal-free catalytic cycle appears to involve an ordered binding sequence of substrate followed by ATP, in contrast to the random, nearly simultaneous binding that takes place with divalent metals. This raises the interesting possibility that the metal-free complex may be a suitable model system for resolving dynamic states, and the transitions between them associated with ATP binding.

■ ASSOCIATED CONTENT

Ⓢ Supporting Information

Crystallographic data collection, refinement, and additional figures. This material is available free of charge via the Internet at http://pubs.acs.org.

■ AUTHOR INFORMATION

Corresponding Author
*E-mail: kovalevskyay@ornl.gov. Phone: 505-310-4184.

Author Contributions
O.G. and A.D. contributed equally to the current study.

Notes
The authors declare no competing financial interest.

■ ABBREVIATIONS

PKAc, catalytic subunit of the protein kinase A; PKI, heat-stable protein kinase inhibitor; SP20, 20-residue peptide substrate

■ REFERENCES

(1) Adams, J. A. (2001) Kinetic and catalytic mechanisms of protein kinases. *Chem. Rev. 101*, 2271−2290.

(2) Johnson, D. A., Akamine, P., Radzio-Andzelm, E., Madhusudan, and Taylor, S. S. (2001) Dynamics of cAMP-dependent protein kinase. *Chem. Rev. 101*, 2243−2270.

(3) Shabb, J. B. (2001) Physiological substrates of cAMP-dependent protein kinase. *Chem. Rev. 101*, 2381−2411.

(4) Taylor, S. S.; Buechler, J. A.; Knighton, D. R. (1990) in *Peptides and protein phosphorylation* (Kemp, B. E., Ed.), pp 1−41, CRC, Boca Raton, FL.

(5) Masterson, L. R., Cheng, C., Yu, T., Tonelli, M., Kornev, A., Taylor, S. S., and Veglia, G. (2010) Dynamics connect substrate recognition to catalysis in protein kinase A. *Nat. Chem. Biol. 6*, 821−828.

(6) Masterson, L. R., Shi, L., Metcalfe, E., Gao, J., Taylor, S. S., and Veglia, G. (2011) Dynamically committed, uncommitted, and quenched states encoded in protein kinase A revealed by NMR spectroscopy. *Proc. Natl. Acad. Sci. U.S.A. 108*, 6969−6974.

(7) Sims, P. C., Moody, I. S., Choi, Y., Dong, C., Iftikhar, M., Corso, B. L., Gul, O. T., Collins, P. G., and Weiss, G. A. (2013) Electronic measurements of single-molecule catalysis by cAMP-dependent protein kinase A. *J. Am. Chem. Soc. 135*, 7861−7868.

(8) Grant, B., and Adams, J. A. (1996) Pre-steady-state kinetic analysis of cAMP-dependent protein kinase using rapid quench flow techniques. *Biochemistry 35*, 2022−2029.

(9) Lew, J., Taylor, S. S., and Adams, J. A. (1997) Identification of a partially rate-determining step in the catalytic mechanism of cAMP-dependent protein kinase: A transient kinetic study using stopped-flow fluorescence spectroscopy. *Biochemistry 36*, 6717−6724.

(10) Shaffer, J., and Adams, J. A. (1999) An ATP-linked structural change in protein kinase A precedes phosphoryl transfer under physiological magnesium concentrations. *Biochemistry 38*, 5572−5581.

(11) Cox, S., Radzio-Andzelm, E., and Taylor, S. S. (1994) Domain movements in protein kinases. *Curr. Opin. Struct. Biol. 4*, 893−901.

(12) Shaffer, J., and Adams, J. A. (1999) Detection of conformational changes along the kinetic pathway of protein kinase A using a catalytic trapping technique. *Biochemistry 38*, 12072−12079.

(13) Armstrong, R. N., Kondo, H., Granot, J., Kaiser, E. T., and Mildvan, A. S. (1979) Magnetic resonance and kinetic studies of the manganese(II) ion and substrate complexes of the catalytic subunit of adenosine 3′,5′-monophosphate dependent protein kinase from bovine heart. *Biochemistry 18*, 1230−1238.

(14) Armstrong, R. N., Kondo, H., and Kaiser, E. T. (1979) Cyclic AMP-dependent ATPase activity of bovine heart protein kinase. *Proc. Natl. Acad. Sci. U.S.A. 76*, 722−725.

(15) Bhatnagar, D., Roskoski, R., Jr., Rosendahl, M. S., and Leonard, N. J. (1983) Adenosine cyclic 3′,5′-monophosphate dependent protein kinase: A new fluorescence displacement titration technique for characterizing the nucleotide binding site on the catalytic subunit. *Biochemistry 22*, 6310−6317.

(16) Zheng, J., Trafny, E. A., Knighton, D. R., Xuong, N. H., Taylor, S. S., Ten Eyck, L. F., and Sowadski, J. M. (1993) 2.2 Å refined crystal structure of the catalytic subunit of cAMP-dependent protein kinase complexed with MnATP and a peptide inhibitor. *Acta Crystallogr. D49*, 362−365.

(17) Zheng, J., Knighton, D. R., Ten Eyck, L. F., Karlsson, R., Xuong, N.-h., Taylor, S. S., and Sowadski, J. M. (1993) Crystal structure of the catalytic subunit of cAMP-dependent protein kinase complexed with MgATP and peptide inhibitor. *Biochemistry 32*, 2154−2161.

(18) Herberg, F. W., Doyle, M. L., Cox, S., and Taylor, S. S. (1999) Dissection of the nucleotide and metal-phosphate binding sites in cAMP-dependent protein kinase. *Biochemistry 38*, 6352−6360.

(19) Cook, P. F., Neville, M. E., Jr., Vrana, K. E., Hartl, F. T., and Roskoski, R., Jr. (1982) Adenosine cyclic 3′5′-monophosphate dependent protein kinase: Kinetic mechanism for the bovine skeletal muscle catalytic subunit. *Biochemistry 21*, 5794−5799.

(20) Kovalevsky, A. Y., Johson, H., Hanson, B. L., Waltman, M. J., Fisher, S. Z., Taylor, S., and Langan, P. (2012) Low- and room-temperature X-ray structures of protein kinase A ternary complexes shed new light on its activity. *Acta Crystallogr. D68*, 854−860.

(21) Valiev, M., Yang, J., Adams, J. A., Taylor, S. S., and Weare, J. H. (2007) Phosphorylation reaction in cAPK protein kinase − Free energy quantum mechanical/molecular mechanics simulations. *J. Phys. Chem. B 111*, 13455−13464.

(22) Cheng, Y., Zhang, Y., and McCammon, J. A. (2005) How does the cAMP-dependent protein kinase catalyze the phosphorylation reaction: An ab initio QM/MM study. *J. Am. Chem. Soc. 127*, 1553−1562.

(23) Szarek, P., Dyguda-Kazimierowicz, E., Tachibana, A., and Sokalski, W. A. (2008) Physical nature of intermolecular interactions within cAMP-dependent protein kinase active site: Differential transition state stabilization in phosphoryl transfer reaction. *J. Phys. Chem. B 112*, 11819−11826.

(24) Adams, J. A., and Taylor, S. S. (1993) Divalent metal ions influence catalysis and active site accessibility in the cAMP-dependent protein kinase. *Protein Sci. 2*, 2177−2186.

(25) Gerlits, O., Waltman, M. J., Taylor, S., Langan, P., and Kovalevsky, A. (2013) Insights into the phosphoryl transfer catalyzed by cAMP-dependent protein kinase: An X-ray crystallographic study of complexes with various metals and peptide substrate SP20. *Biochemistry 52*, 3721−3727.

(26) Mitchell, R. D., Glass, D. B., Wong, C.-W., Angelos, K. L., and Walsh, D. A. (1995) Heat-stable inhibitor protein derived peptide substrate analogs: Phosphorylation by cAMP-dependent and cGMP-dependent protein kinases. *Biochemistry 34*, 528−534.

(27) Glass, D. B., Cheng, H.-C., Mueller, L. M., Reed, J., and Walsh, D. A. (1989) Primary structural determinants essential for potent inhibition of cAMP-dependent protein kinase by inhibitory peptides corresponding to the active portion of the heat-stable inhibitor protein. *J. Biol. Chem. 264*, 8802−8810.

(28) Minor, W., Cymborowski, M., Otwinovski, Z., and Chruszcz, M. (2006) HKL3000: The integration of data reduction and structure solution − from diffraction images to an initial model in minutes. *Acta Crystallogr. D62*, 859−866.

(29) Sheldrick, G. M. (2008) A short history of SHELX. *Acta Crystallogr. A: Found. Crystallogr. 64*, 112−122.

(30) Adams, P. D., Afonine, P. V., Bunkóczi, G., Chen, V. B., Davis, I. W., Echols, N., Headd, J. J., Hung, L.-W., Kapral, G. J., Grosse-Kunstleve, R. W., McCoy, A. J., Moriarty, N. W., Oeffner, R., Read, R.

J., Richardson, D. C., Richardson, J. S., Terwilliger, T. C., and Zwart, P. H. (2010) PHENIX: A comprehensive Python-based system for macromolecular structure solution. *Acta Crystallogr. D: Biol. Crystallogr. 66*, 213−221.

(31) Emsley, P., Lohkamp, B., Scott, W. G., and Cowtan, K. (2010) Features and development of Coot. *Acta Crystallogr. D66*, 486−501.

(32) Mukherjee, K., Sharma, M., Urlaub, H., Bourenkov, G. P., Jahn, R., Sudhof, T. C., and Wahl, M. C. (2008) CASK functions as a Mg^{2+}-independent neurexin kinase. *Cell 133*, 328−339.

(33) Gibbs, C. S., and Zoller, M. J. (1991) Identification of electrostatic interactions that determine the phosphorylation site specificity of the cAMP-dependent protein kinase. *Biochemistry 30*, 5329−5334.

(34) Gibbs, C. S., and Zoller, M. J. (1991) Rational scanning mutagenesis of a protein kinase identifies functional regions involved in catalysis and substrate interactions. *J. Biol. Chem. 266*, 8923−8931.

(35) Aimes, R. T., Hemmer, W., and Taylor, S. S. (2000) Serine-53 at the tip of the glycine-rich loop of cAMP-dependent protein kinase: Role in catalysis, P-site specificity, and interaction with inhibitors. *Biochemistry 39*, 8325−8332.

(36) Whitehouse, S., and Walsh, D. A. (1983) $MgATP^{2-}$-dependent interaction of the inhibitor protein of the cAMP-dependent kinase with the catalytic subunit. *J. Biol. Chem. 258*, 3682−3692.

(37) Madhusudan, Trafny, E. A., Xuong, N.-H., Adams, J. A., Ten Eyck, L. F., Taylor, S. S., and Sowadski, J. M. (1994) cAMP-dependent protein kinase: crystallographic insights into substrate recognition and phosphotransfer. *Protein Sci. 3*, 176−187.

(38) Qamar, R., and Cook, P. F. (1993) pH dependence of the kinetic mechanism of the adenosine 3′,5′-monophosphate dependent protein kinase catalytic subunit in the direction of magnesium adenosine 5′-dophosphate phosphorylation. *Biochemistry 32*, 6802−6806.

(39) Storer, A. C., and Cornish-Bowden, A. (1976) Concentration of $MgATP^{2-}$ and other ions in solution. *Biochem. J. 159*, 1−5.

(40) Alberty, R. A., Smith, R. M., and Bock, R. M. (1951) The apparent ionization constants of the adenosinephosphates and related compounds. *J. Biol. Chem.*, 425−434.

(41) Wilson, J. E., and Chin, A. (1991) Chelation of divalent cations by ATP, studied by titration calorimetry. *Anal. Biochem. 193*, 16−19.

(42) Montenegro, M., Masgrau, L., Gonzalez-Lafont, A., Lluch, J. M., and Garcia-Viloca, M. (2012) Influence of the enzyme phosphorylation state and the substrate on PKA enzyme dynamics. *Biophys. Chem. 161*, 17−28.

(43) Madhusudan, Akamine, P., Xuong, N.-H., and Taylor, S. S. (2002) Crystal structure of a transition state mimic of the catalytic subunit of cAMP-dependent protein kinase. *Nat. Struct. Biol. 9*, 273−277.

(44) Blow, D. (2000) So do we understand how enzymes work? *Structure 8*, R77−R81.

(45) Jencks, W. P. (1986) *Catalysis in Chemistry and Enzymology*, Dover Publ, New York.

(46) Admiraal, S. J., and Herschlag, D. (1995) Mapping the transition state for ATP hydrolysis: implications for enzymatic catalysis. *Chem. Biol. 2*, 729−739.

(47) Montenegro, M., Garcia-Viloca, M., Lluch, J. M., and Gonzalez-Lafont, A. (2011) A QM/MM study of the phosphoryl transfer to the Kemptide substrate catalyzed by protein kinase A. The effect of the phosphorylation state of the protein on the mechanism. *Phys. Chem. Chem. Phys. 13*, 530−539.

(48) Creanga, C., and El Murr, N. (2011) Development of new disposable NADH biosensors based on NADH oxidase. *J. Electroanal. Chem. 656*, 179−184.

(49) Salih, S. G., Khan, J. A., and Newton, R. P. (1988) Cytidine 3′,5′-cyclic monophosphate phosphodiesterase: Immunoreactivity and differential sensitivity to endogenous effectors. *Biochem. Soc. Trans. 16*, 774−775.